GeoArabia, Vol. 13, No. 2, 2008
Gulf PetroLink, Bahrain

Design of a P-wave seismic vibrator with advanced performance

Zhouhong Wei

ABSTRACT

For optimal seismic imaging, the vibroseis method requires the vibrator to generate synchronous, repeatable sweeps over a broad frequency range and output the ground-force energy with minimum harmonic distortion. This requires re-evaluating each element of the vibrator system to ensure that it contributes to the success of the method. Key factors that cause the vibrator to suffer from severe harmonic distortion are fluctuations in the hydraulic power supply pressure, flexing of the baseplate, coupling or loading between the baseplate and the ground, nonlinear servo-valve flow-pressure characteristics, and servo-valve characteristics near null. This paper examines these factors and describes the design of a new P-wave vibrator by ION (previously I-O) to improve seismic resolution. Experimental results demonstrate that the newly designed vibrator dramatically reduces harmonic distortion in the ground-force signal under various coupling conditions, particularly on hard and uneven ground. With the high-frequency controller and Pelton DR valve, a broad-band sweep frequency is achieved. Cavitations in the supply pressure, a long-standing problem in vibrator mechanics, are almost completely eliminated.

INTRODUCTION

The vibroseis system constitutes the primary land seismic source for imaging the subsurface, for both exploration and reservoir characterization. Ideally, the vibroseis system should generate a broadband seismic wavelet that is repeatable from shotpoint to shotpoint (Chapman et al., 1981). Improved repeatability of the source signature helps resolve statics corrections, resulting in more coherent reflectors in the final stack. In order to achieve these objectives, it is key to maintain good coupling between the force exerted by the vibrator's baseplate and the ground over a wide range of swept frequencies (Figures 1 and 2). In typical Middle Eastern terrains, this objective is particularly challenging due to highly variable surface conditions, commonly consisting of dunes, jabals, karsts, and wadis (Bridle et al., 2006; Ley et al., 2006; Al-Ali and Verschuur, 2006; Baetan and Van Der Heijdan, 2008). In these rough terrains, the Earth's hardground surface is frequently overlaid with loose gravel or sand, resulting in a changeable contact area and a degradation of the baseplate-Earth coupling effectiveness. Vibrating on these surfaces generates harmonic distortions and baseplate flexural vibrations at higher sweep frequencies, resulting in poor repeatability and distorted source signatures.

Nonlinear effects in the vibrator's hydraulic system and the ground's response, cause harmonic distortion to be generated by the vibrator's baseplate. These harmonics, particularly the second and third harmonics, appear as *harmonic ghosts* in the correlated data and are difficult to suppress in processing. Reducing source-generated harmonic distortion not only reduces coherent noise, but also enables the vibrator to shake harder and produce more down-going energy.

The vibrator's frequency bandwidth is another important factor in resolving finer details in the seismic image. Typically, vibrators are most effective in radiating energy between 15 and 50 Hz, corresponding to a maximum resolution of 50 m in subsurface thickness. For frequencies below 10 Hz, the vibrator cannot produce sufficient force due to mechanical and hydraulic constraints (e.g., the reaction mass peak-to-peak stroke and the peak-decoupling force). At these low frequencies, the vibrator output suffers severe harmonic distortion while the energy goes to correlation noise rather than enhancing the signal. For higher frequencies, which may range from 50 to 150 Hz, the vibrator output energy is limited due to the narrow frequency bandwidth of the servo-valve system and the low rigidity of the baseplate structure. Nevertheless, Baetan and Van Der Heidan (2008) have shown in recent experiments in Oman, that energy of up to 150 Hz can be recorded from reflectors at depths of 2,000 m.

This paper examines the mechanical limitations of conventional seismic vibrators and describes a new ION (previously I-O) P-wave vibrator that significantly improves seismic resolution. The discussion is presented in five sections. The first briefly describes the seismic vibrator and ground force. The next three sections discuss the hydraulic power supply pressure system, vibrator baseplate flexure, and the servo-valve system and high-frequency controller. The final two sections show the experimental results and state the conclusions.

SEISMIC VIBRATOR AND GROUND FORCE

The seismic vibrator is an electronically controlled, hydro-mechanical system driven by a servo-valve assembly (Figure 1). The input to the system, the *hydraulic power supply*, drives the vibroseis system by pumping oil into the *main-stage servo-valve assembly* and then across the *baseplate piston*. The power supply typically consists of a diesel engine that drives pumps, a fluid reservoir, a pressure regulator, safety relief valves, hydraulic filters, an oil cooler and accumulators.

The output of the system, the *ground force* (Fg, Figure 1 and Table 1), is exerted by the vibrator's baseplate against the Earth's surface; it is the compressive stress field integrated over the contact area. The ground force varies as a function of frequency, attaining a maximum at the *resonant frequency* (fo), which for mud and sand terrains is about 25 and 35 Hz, respectively (Figure 2a). The resonant frequency depends on the sum (Ms) of the *baseplate mass* (Mb), *captured ground mass* (Mg) and *ground stiffness* (Gs) (Figure 2b).

Traditionally, the seismic trace is computed by cross-correlating the recorded data with the reference sweep that drives the vibroseis system. Better seismic resolution, however, can be achieved by using the actual ground force as the reference to deconvolve the recorded data. To measure the actual force, accelerometers are mounted on the vibrator structure to record the accelerations of the baseplate (Ab) and the reaction mass (Ar). For ION's AHV-IV vibrator, the two accelerometers are mounted on the top-crossing of the baseplate stilt structure and the top of the reaction mass (Figure 1).

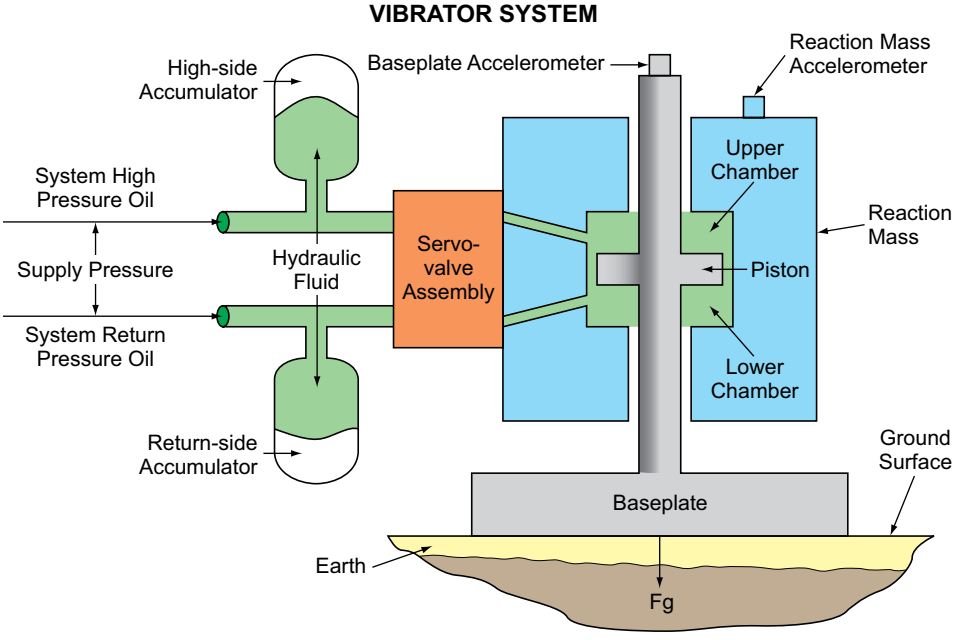

Figure 1: Simplified schematic cross-section of the vibroseis system showing the hydraulic power supply, servo-valve assembly, reaction mass, piston and baseplate. The piston is positioned in a cylindrical bore inside the reaction mass, and is rigidly attached to the baseplate. High-pressure hydraulic fluid is alternately fed into the upper and lower chambers and drives the reaction mass up-and-down. The force acting on the reaction mass is equally and oppositely applied to the piston, causing the ground force (Fg) to be transmitted into the ground.

Table 1

Abbreviations	Definitions
Ab	Acceleration of baseplate (meter/second^2)
Ar	Acceleration of reaction mass (meter/second^2)
dB	Decibel, relative amplitude ratio (unitless)
Fg	Ground force (Newtons)
f	Frequency (Hertz)
fo	Resonant frequency of vibroseis system (Hertz)
Gs	Ground stiffness (Newton/meter); for ION's AHV-IV vibrator Gs is 8.3×10^7 N/m for mud, and 1.42×10^8 N/m for sand.
Gv	Ground viscosity (Newton-second/meter)
$[G_f(s)]$, $[G_{ffd}(s)]$, $[G_s(s)]$	Transfer functions in Control System (see Figure 5)
Hs	Hydraulic oil stiffness (Newton/meter)
Hv	Hydraulic oil viscosity (Newton-second/meter)
Hz	Hertz (cycles/second)
$[H_f(s)]$	Transfer function in Control System (see Figure 5)
K	Orifice flow coefficient (meter^3/second x bar $^{1/2}$)
Ms	Combined mass of baseplate and captured ground (kilogram); for ION's AHV-IV vibrator Ms is 3,321 Kg for mud, and 3,045 Kg for sand.
Mb	Mass of the baseplate (kilogram)
Mg	Mass of captured ground (kilogram)
Mr	Mass of reaction mass (kilogram)
Ps	Supply pressure (bar) = System high pressure (bar) - Return pressure (bar)
PL	Load or differential pressure (bar)
QL	Hydraulic load flow (meter^3/second)
U	Force control variable (see Figure 5)
U_{ffd}	Frequency control variable (see Figure 5)
Xv	Opening of the main-stage servo-valve (meter)

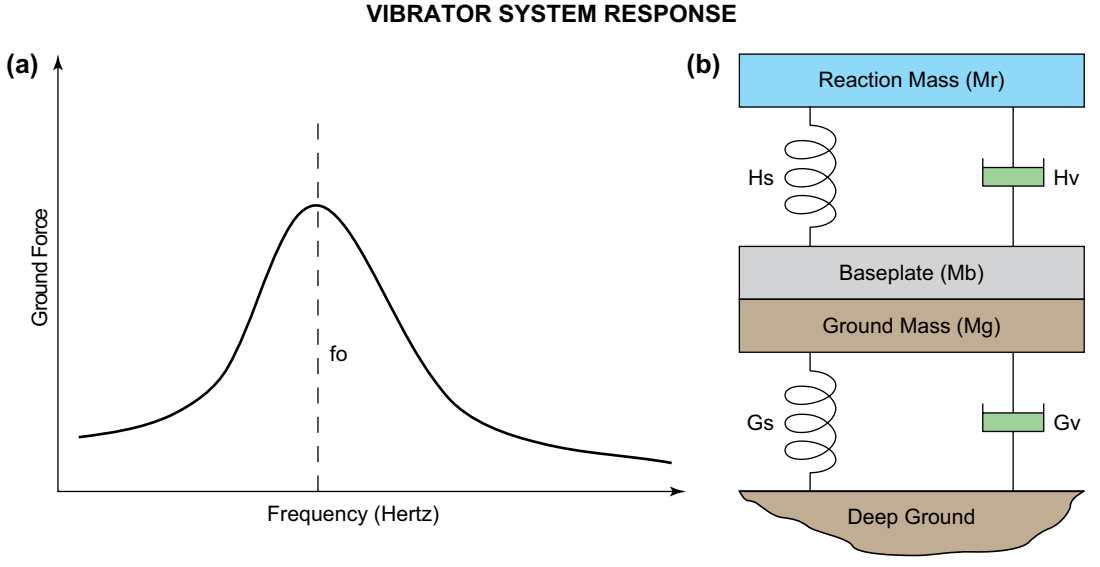

Figure 2: (a) Typical ground-force versus frequency response of the vibrator-ground system. The *resonant frequency* (fo) in conventional vibrators typically ranges between 15 and 35 Hz. (b) A mass-spring-dashpot mechanical model is presented to describe the vibrator-ground system. The captured ground is represented by its stiffness (Gs), viscosity (Gv) and mass (Mg). The baseplate and reaction mass are represented by masses Mb and Mr, respectively. The impacts of the hydraulic oil stiffness (Hs) and viscosity (Hv) are negligible due to incompressible hydraulic flow. The differential pressure driving the reaction mass up-and-down is applied equally and oppositely to the baseplate, and generates the ground force.

The actual ground force is estimated as follows (Sallas, 1984):

$$- Fg = Mr \times Ar + Mb \times Ab \qquad (1)$$

This approximation assumes that the baseplate acts as a rigid body, which is normally true only below 50 Hz. In fact, when accelerometers are placed at different locations within the baseplate, different dynamic motions are recorded, implying that this approximation is only representative in a narrow frequency bandwidth.

Poor baseplate coupling causes uneven loading and large changes in fluid-flow requirements. In such conditions, the fluid in the main-stage servo-valve (Figure 1) flows in a turbulent and fluctuating regime. Large supply-pressure ripples modulate the fluid-flow output of the servo-valve, causing harmonic distortion (dominated by the second harmonics) in the pressure across the baseplate piston. This distorts the accelerations of the reaction mass and baseplate, as well as the ground force (calculated using the weighted-sum method). These issues were resolved in the design of a new vibrator system and are discussed in the next sections.

HYDRAULIC POWER SUPPLY PRESSURE SYSTEM

The hydraulic power supply system maintains a *system high pressure* (224 bars) and a *return pressure* (17 bars) (Figures 2 and 3). The *supply pressure* (Ps) to the main-stage servo-valve is the difference between these (207 bars). The *hydraulic load flow* (QL) is delivered through the servo-valve control ports to yield a *load pressure* (or a *differential pressure*, PL) across the baseplate piston. This is controlled by the opening of the servo-valve (Xv) (Merritt, 1967):

$$QL = KXv\sqrt{Ps - \frac{Xv}{|Xv|}PL} \qquad (2)$$

where K is the *orifice flow coefficient*.

Equation (2) shows that hydraulic load flow is related to the square root of the supply pressure, the opening size of the main-stage valve and the load pressure. This nonlinear relationship characterizes the main source for the odd harmonic distortion, which is dominated by the third harmonic, especially at low frequencies. At low frequencies, because greater hydraulic flow is required to reach the target ground force, the spool of the main-stage valve has to travel further. The resulting large opening in the valve creates a strong nonlinearity such that the load flow and ground force are severely contaminated with odd harmonics.

The four-way servo-valve operates as a supply-flow mechanism that resembles a full-wave rectified sine wave (i.e. absolute values of a sine wave), and is rich in second harmonics. Because the pump is generally positioned some distance from the servo-valve inlet, the intervening hoses and passageways constitute a high-impedance pathway between them. When the flow fluctuates, this impedance tends to isolate the pump's output, causing pressure ripples at the servo-valve inlet.

In most cases, to mitigate this problem, hydraulic accumulators are located near the servo-valve. These filter pressure pulsations from pumps and harmonic ripples from servo-valves and provide additional pressurized fluid to meet peak-flow demands. In many vibrators, however, the accumulators are too far from the point-of-use to be effective. Often, high-frequency pressure spikes are created when the valve switches through zero position. This fluid *hammer effect* can be large enough to cause gas bubbles (cavitations) to form in the fluid as the system return pressure approaches zero bars (Figure 3). When the bubbles collapse inside the servo-valve, they cause severe damage, including pitting of its spools and other components. Harmonics in the supply pressure corrupt the differential pressure (Equation 2), resulting in high turbulence (recognized as an audible buzz in the servo-valve system).

To overcome these problems, we have designed a new reaction-mass system. This redesign involves using shorter supply lines for the hydraulic fluid-flow hoses and flow passages in the reaction mass. In addition, the sizes of passageways were recalibrated to minimize restrictions to flow, and the accumulators were repositioned more effectively.

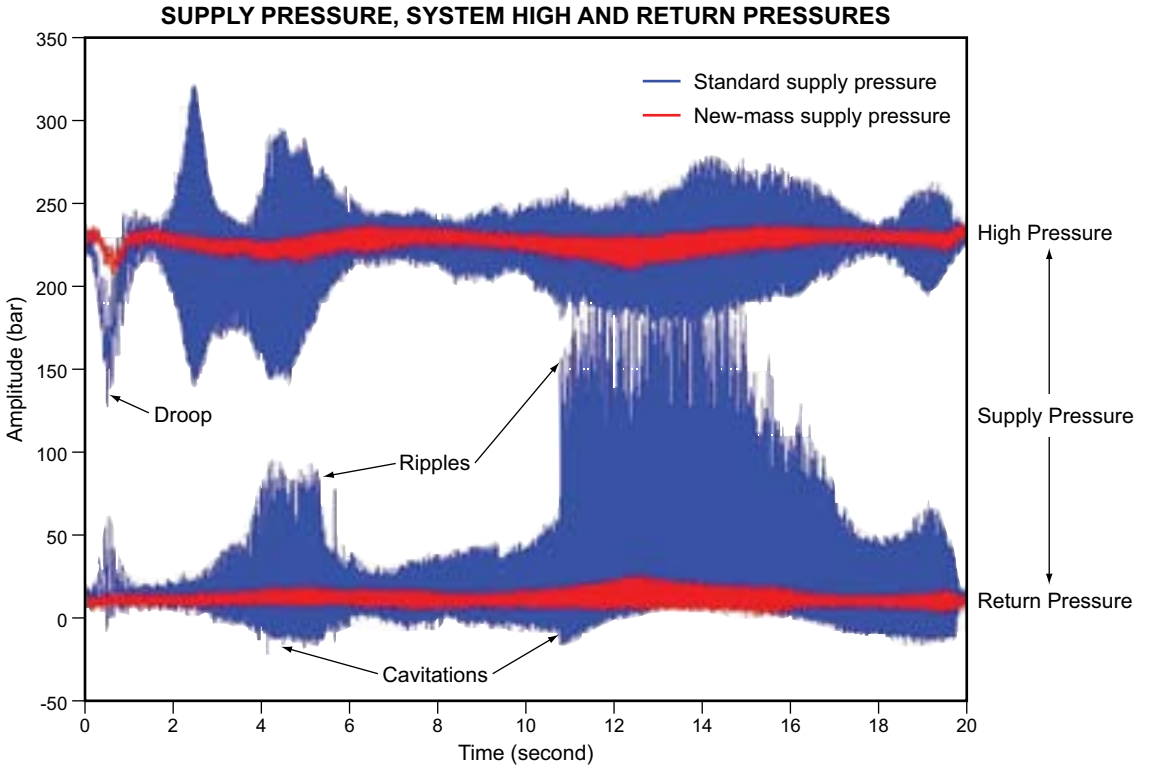

Figure 3: Comparison of the standard supply pressure (blue) and the new-mass supply pressure (red) on ION's AHV-IV vibrator performing a 1 to 201 Hz linear sweep in 20 seconds. The new design dramatically reduced pressure ripples in both system high and return pressures. Cavitations in the system return pressure and the 'droop' at low frequencies in the system high pressure were eliminated.

Figure 3 compares the standard (blue curve) and new-mass supply pressure (red curve) performances for ION's AHV-IV vibrator performing a linear 1 to 201 Hz sweep in 20 seconds. Hammer effects caused by cavitations are recognized by a drop in the return pressure below zero, followed by large spikes. Ripples are represented by large oscillations in the standard supply pressure. Near the initiation of the sweep, the 'droop' in the system high pressure is reduced by two-thirds in the new design. The ripples and cavitations present throughout the sweep have been virtually eliminated. Also of note is the stability of the measured ground force at high frequencies.

VIBRATOR BASEPLATE FLEXURE

When a vibrator shakes, particularly at higher frequencies, the baseplate bends, flexes, and rocks back-and-forth in a complex manner. Different parts of the baseplate move separately in response to ground-related nonlinearities, which, in turn, causes turbulent flow in the hydraulic system and instability in the servo-valve assembly. The estimate of the actual ground force using the weighted-sum (Equation 1) becomes inaccurate at high frequencies due to distortion by even harmonics. We overcame this limitation by stiffening the baseplate, which involved changing the structural shapes of its mechanical components. The new baseplate is 2.5 times more stiff than the standard one and only 5% heavier.

To compare the performance of the standard and new baseplates, we designed an experiment using a 1 to 201 Hz, 20-second sweep and load-cell sensors. The load cells were positioned between the baseplate and the ground. They are very rigid and provide a direct measurement of the actual ground force. Figure 4 shows the magnitude ratio and phase spectra (frequency-response or bode plots) of the ground force calculated by the weighted-sum method compared to the ground force measured by the load-cell sensors. The spectra were calculated using the weighted-sum ground force as the output and the actual ground force measured by load cells as the input. In theory, if the weighted-sum and measured ground forces are equal, the magnitude ratio spectrum is 0 dB and the phase spectrum remains at zero degree.

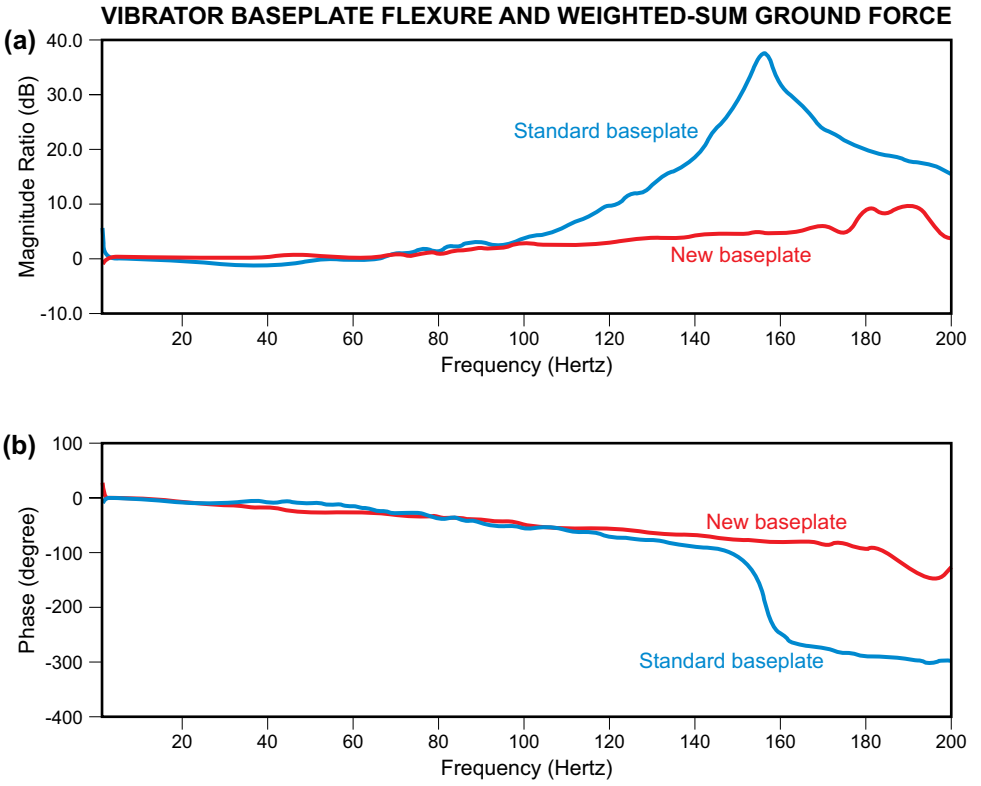

Figure 4: (a) The weighted-sum ground force response in the frequency domain is used to evaluate the baseplate's rigidity. If the baseplate acts as a true rigid body, the weighted-sum ground force should be equal to the actual ground force, and a zero-dB and zero-phase will be seen in frequency-response plots. Below 80 Hz, the weighted-sum ground force can approximate the true ground force for both baseplates. For frequencies above 80 Hz, the weighted-sum ground force with the standard baseplate overestimates the true ground force, while with the new baseplate, the weighted-sum ground force is valid up to 160 Hz. (b) Phase plot.

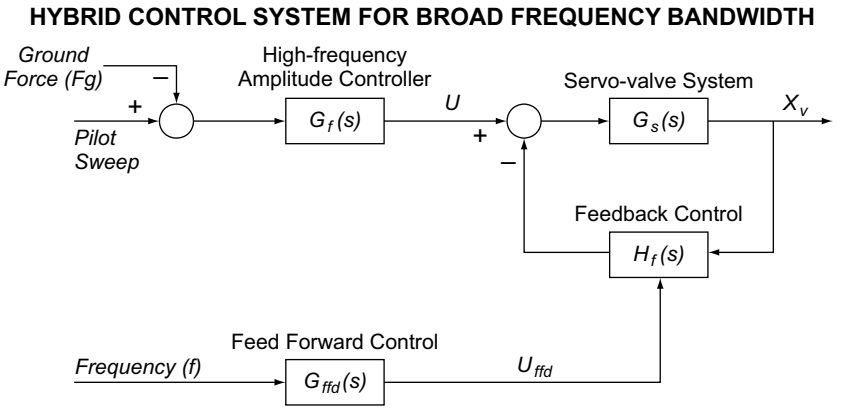

Figure 5: Block diagram showing the digital signal path executed by the Pelton VibPro™ control electronics. Abbreviations in rectangular boxes are transfer functions in the frequency domain, and the "s" in parentheses is the Laplace transform operator. The upper path shows the pilot sweep, which is generated by the Digital Signal Processor (DSP) in VibPro™ control electronics. The ground force (Fg), approximated by the weighted-sum method, is fed back with a minor delay to the DSP. The difference between the pilot sweep and the ground force is then passed to the high-frequency amplitude controller [$G_f(s)$], resulting in the output of the force-control variable (U). It is then passed to the closed-loop servo-valve feedback system, consisting of the servo-valve system [$G_s(s)$] and the feedback control, represented by [$H_f(s)$]. In the lower path, the sweep frequency (f) is passed into the frequency-dependent feed-forward control [$G_{ffd}(s)$]. It generates a control frequency-dependent gain (U_{ffd}), which adjusts the feedback control [$H_f(s)$]. The final output (Xv) is the displacement of the servo-valve assembly.

For the standard baseplate, the estimated and measured ground forces were approximately equal below 80 Hz (using an alternative definition of bandwidth where the error magnitude approaches 3 dB from the zero dB line). The estimated phase of the standard baseplate lagged that of the measured ground force by about 90° at 80 Hz. In contrast, the new baseplate had a better match between the weighted-sum and measured ground forces up to 160 Hz, at which the phase approached -90°.

SERVO-VALVE SYSTEM AND HIGH-FREQUENCY CONTROLLER

Typically, the reaction mass and baseplate assembly of a seismic vibrator is driven by a hydraulic servo-valve system consisting of a Moog 760-928A pilot servo-valve and an Atlas 240H main-stage servo-valve. If supported by the control electronics, the Pelton DR valve can be installed between the pilot servo-valve and the main-stage servo-valve. With this option, the main-stage servo-valve is converted from flow-control to pressure-control (Ruest, 1993).

In Equation (2), assuming the supply pressure (Ps) is constant, the dynamics of the main-stage servo-valve opening (Xv) significantly impact the load flow (QL). Once the Pelton DR valve is enabled, the main-stage servo-valve works in pressure-control mode such that the differential pressure (PL) acts as a feedback signal. It is then fed back through flow passages in the DR valve plate to adjust the main-stage servo-valve opening. This feedback optimizes the servo-valve openings and reduces turbulence in the load flow, rendering the ground-force control more accurate. In addition, the baseplate and Earth resonances are dampened.

The high-frequency controller consists of software embedded in Pelton VibPro™ control electronics. In operation, the Pelton control electronics are in the vibrator driver's cab. The control electronics are connected to the servo-valve assembly through cables and control the motion of the servo-valve assembly. Figure 5 describes the high-frequency controller. Overall control of the servo-valve system [$G_s(s)$] is accomplished with three control algorithms: the high-frequency amplitude controller [$G_f(s)$], the feed-forward controller [$G_{ffd}(s)$] and the feedback controller [$H_f(s)$]. In the calibration process performed before operating the vibrator, the servo-valve system is automatically stabilized by the feedback controller. When the vibrator shakes, the feed-forward controller outputs a varying gain to adjust the feedback controller. The adjustment is based on the frequency of the sweep and attenuates high-frequency resonances in the servo-valve.

Figure 6 compares the frequency responses of the servo-valve closed loop of a standard controller, and the new high-frequency controller, with the Pelton DR valve disabled. With the new controller, the resonant peak at around 200 Hz was dramatically damped (Figure 6a). Using the alternative definition of bandwidth (where the error magnitude approaches -3 dB), the closed-loop frequency

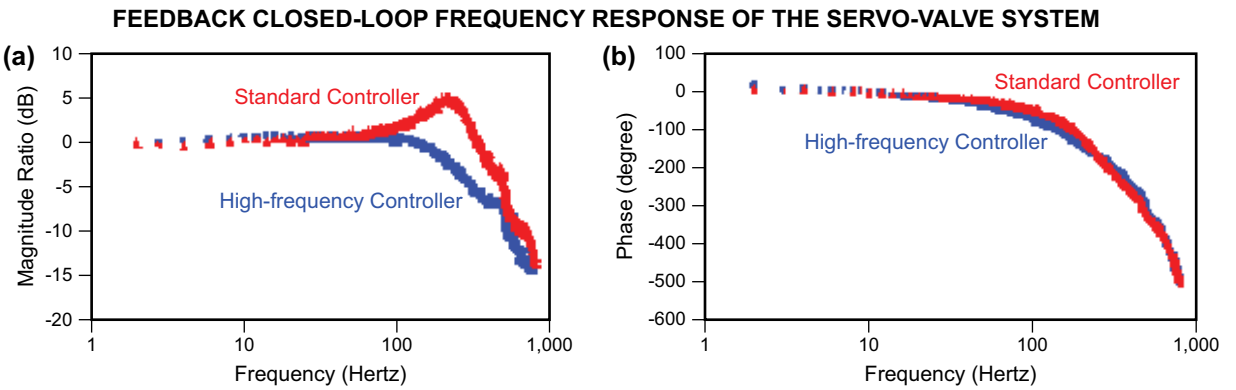

Figure 6: Servo-valve closed-loop frequency response: (a) magnitude ratio plot, (b) phase plot. The servo-valve closed-loop frequency response of a standard controller is compared with that of the new high-frequency controller. The high-frequency controller offers advantages in suppressing significant resonances at 200 and 450 Hz. With dampened resonances, a smooth servo-valve system dynamic response is achieved.

Figure 7: The vibrator is on a gravel track in Sealy, Texas, USA. The gravel track is about 25.4 cm thick and overlies Texas black clay. The gravel track is fairly flat and the vibrator is well-coupled with the ground surface.

bandwidth was extended to 200 Hz. At this bandwidth, the phase was shifted by 90°, so there was still some phase margin for phase-loop control. Figure 6a shows that a resonant peak at 450 Hz was suppressed, indicating that very high-frequency resonances were damped.

High gain at low frequencies is good for tracking control and disturbance-rejection. Low gain at high frequencies is good for phase-margin and control-stability (Schinstock et al., 2006; Wei and Schinstock, 2005). These principles, applied in designing the high-frequency amplitude controller, suppressed the high-frequency resonances due to baseplate flexure. With this design, a broad-bandwidth servo-valve system was achieved (Figure 6a).

EXPERIMENTAL RESULTS

Figure 7 shows an example of a test conducted with ION's AHV-IV vibrator with the new mass and baseplate located on a gravel track at the ION testing facility in Sealy, Texas, USA. The gravel track is about 25.4 cm thick and overlies Texas black clay. A linear sweep from 5 to 105 Hz in 20 seconds was performed at 75% force. Although the baseplate was well-coupled with the ground, small areas remained beneath it that were not in full contact. The vibrator was controlled by the control electronics with the high-frequency controller.

Figure 8 is the frequency-time plot of measured ground forces using the standard AHV-IV and new AHV-IV vibrators. On the gravel track, a dramatic reduction in the harmonic distortion at low to mid-range frequencies was measured. The improvement at higher frequencies was less pronounced. In general, there were improvements in the uniformity and consistency of the fundamental content of the ground force with the new mass and baseplate structure. Each harmonic shows a reduction in intensity (about 10 dB), especially the second and third harmonics (Figure 8).

Figure 9 documents a test of an extremely uneven loading condition. The baseplate was situated partially on flat concrete and partially on a ramp, with an air gap between a section of the baseplate and the ground. A 10-second, 5 to 85 Hz linear sweep was performed at 75% force. The attributes of the frequency-time plots of the ground force harmonic distortion (Figure 10) remained similar to those of the gravel track (Figure 8). The overall uniformity and consistency of the fundamental content of the ground force was greatly improved. Even more encouraging, the harmonic distortion

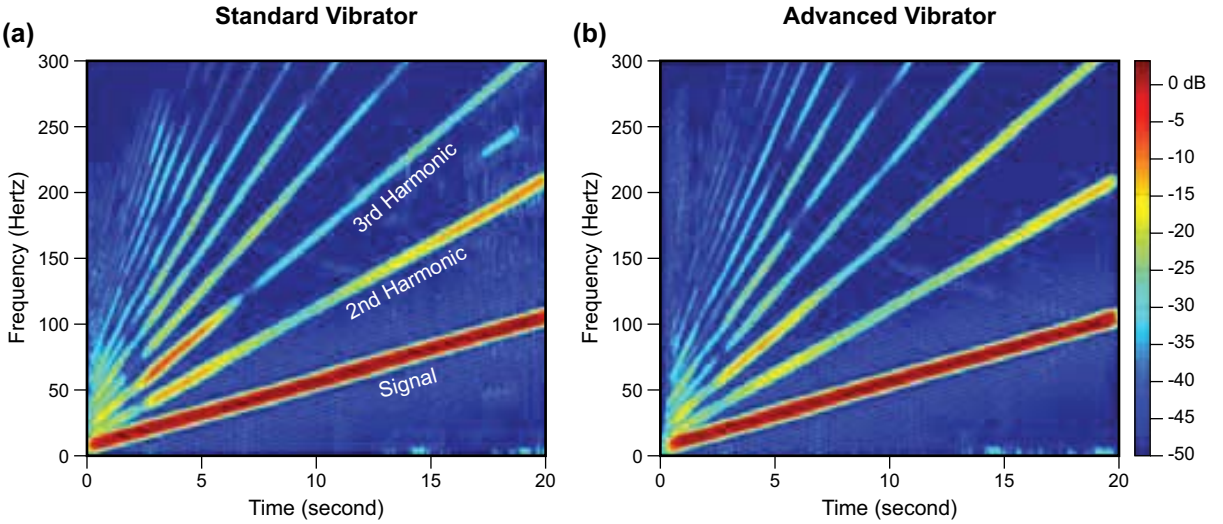

Figure 8: Frequency-time representation of the weighted-sum ground force; (a) Standard AHV-IV vibrator, and (b) AHV-IV vibrator with the new mass and baseplate system. On the gravel track, with the AHV-IV vibrator equipped with the new mass and baseplate, a significant reduction in the harmonic distortion at low to mid-range frequencies was measured. The fundamental content in the ground force was more uniform and consistent. Overall, an improvement of 10 dB-down was seen towards reducing the harmonic distortion.

Figure 9: The vibrator is on concrete in Sealy, Texas, USA. The baseplate was placed partially on flat concrete and partially on a ramp with an air gap between a section of the baseplate and the ground. The purpose was to create an uneven loading so that complex rocking motions would be generated during vibration.

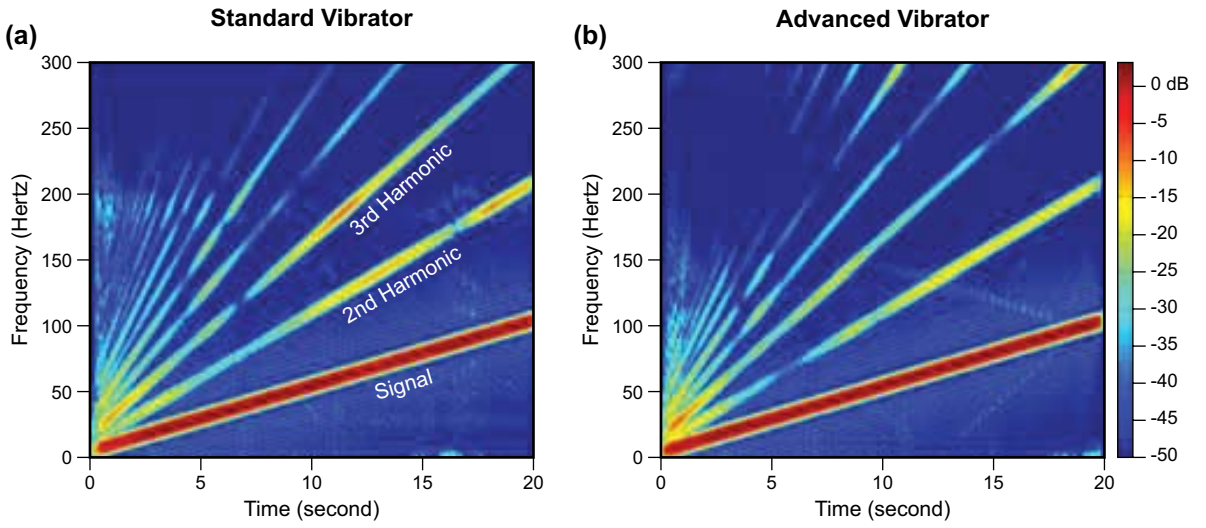

Figure 10: Frequency-time representation of the weighted-sum ground force; (a) Standard AHV-IV vibrator, and (b) AHV-IV vibrator with the new mass and baseplate system. The overall uniformity and consistency of the fundamental content in the ground force was greatly improved. Even more encouraging, the harmonic distortion was significantly reduced throughout the majority of mid-range and high frequencies. In particular, there was a dramatic reduction in the magnitude of the second harmonic distortion at the mid-range and high-end of the sweep. Overall, the third harmonic distortion was also reduced.

was significantly reduced throughout most of the mid-range and high frequencies. Again, there was a reduction in the magnitude of individual harmonics and in particular, the overall noise at the mid-range and high-end of the sweep was adequately compensated.

Figure 11 shows another example with the AHV-IV vibrator located on load cells, where the actual ground force can be measured. Under the baseplate, eight evenly distributed load cells were mounted on the concrete, each having a small contact area. On the top of each cell, two pieces of rubber pad protected it from metal-to-metal contact, resulting in good coupling to the baseplate. The flexural vibration and complex rocking of the baseplate were severe. A linear sweep from 5 to 105 Hz in 10 seconds was performed at 70% force.

Figure 12 shows frequency-time plots of the measured ground forces using the standard AHV-IV vibrator and new AHV-IV vibrator. On load cells, all harmonics show a dramatic reduction in intensity, especially the second and third ones. A harmonic distortion reduction at mid-range to higher frequencies was observed; the harmonics and noise at lower frequencies were also clearly reduced. The uniformity and consistency of the fundamental content of the ground force was significantly enhanced. Overall, the vibrator equipped with the new mass and baseplate system performed much better.

Figure 13 shows the frequency-time plots of the weighted-sum ground force using the standard and new AHV-IV vibrators. The standard vibrator was controlled using standard control electronics while the new vibrator used the high-frequency controller. The Pelton DR valve was installed and enabled. The two vibrators were placed on a flat gravel track where the baseplates were well-coupled and performed a linear sweep from 5 to 250 Hz in 20 seconds at 70% drive force. Figure 13a shows that with the standard controller, oscillations of the servo-valve began at 11 seconds around 150 Hz. At the end of the sweep from 18 to 20 seconds (230 to 250 Hz), the servo-valve system was completely unstable and strong noise was produced. In contrast, Figure 13b demonstrates that the servo-valve was stable for the entire sweep frequency band with the high-frequency controller. Moreover, the fundamental content of the ground force was enhanced, particularly at low frequencies, due to high-gain control. Because the high gain was applied at low frequencies, the good tracking performance was achieved for the fundamental amplitude of the ground force and the phase. Harmonic distortions, especially the second and third harmonics, were significantly suppressed.

Figure 11: The vibrator is on load cells in Sealy, Texas, USA. A total of eight load cells were mounted on the concrete and evenly distributed beneath the baseplate. Two small rubber pads were placed on top of each load cell to protect it from metal-to-metal contact. Under this loading condition, the baseplate was well-coupled with load cells but the contact area was small. The flexural vibration and complex rocking of the baseplate were severe.

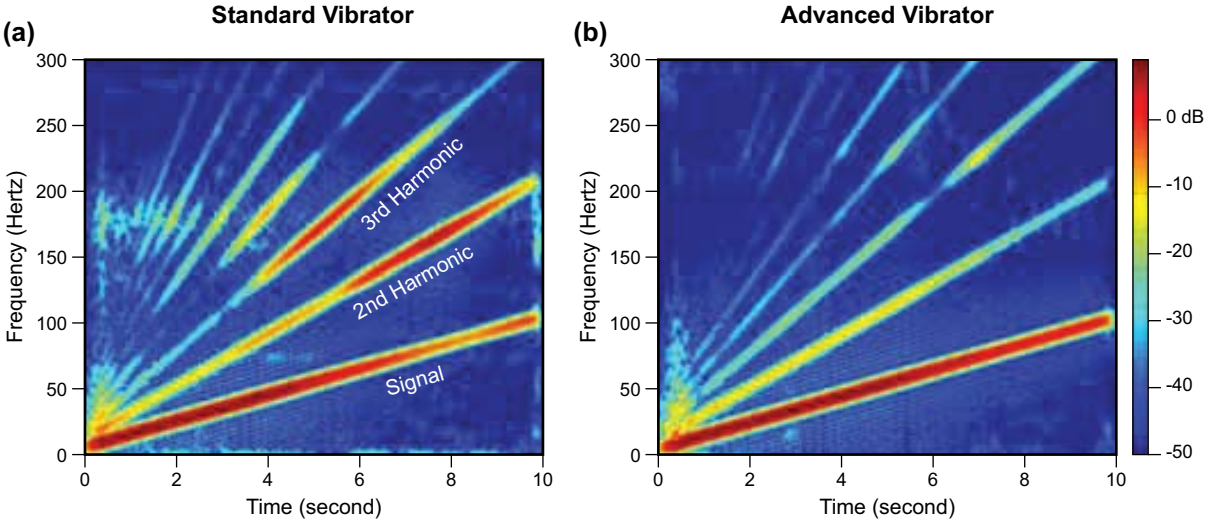

Figure 12: Frequency-time representation of the measured ground force; (a) Standard AHV-IV vibrator, and (b) AHV-IV vibrator with the new mass and baseplate system. On load cells, all harmonics show a dramatic reduction in intensity, especially the second and third harmonics. A harmonic distortion reduction at mid-range to higher frequencies was observed. The harmonics and noise at lower frequencies were also clearly reduced. The uniformity and consistency of the ground force was significantly enhanced. Overall, the vibrator equipped with new mass and baseplate system performed much better.

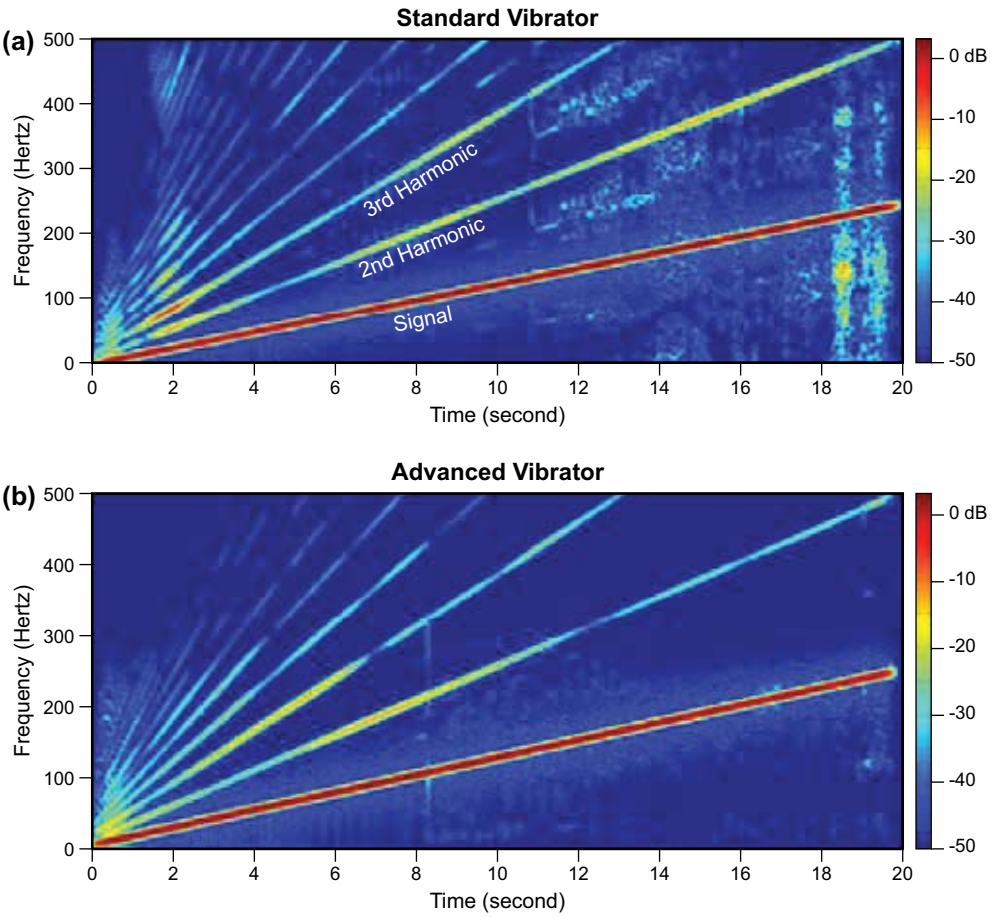

Figure 13: Frequency-time representation of the weighted-sum ground force on a gravel track in Waller, Texas; (a) Standard AHV-IV vibrator; and (b) AHV-IV vibrator with the new mass and baseplate system.

Figure 14 illustrates the frequency-time plots of the measured ground force using load-cell sensors. The standard AHV-IV vibrator used the standard control electronics while the new mass and baseplate vibrator used the high-frequency controller. The Pelton DR valve was turned on and was in working mode. The vibrators performed a linear sweep from 5 to 200 Hz in 20 seconds at 70% drive force. Figure 14 clearly shows that the fundamental content of the ground force produced by both vibrators decreased with increasing frequency. This implies that the weighted-sum ground force method overestimates the actual ground force at high frequencies. Figure 14a shows that with the standard controller, at 16 seconds (around 160 Hz), the servo-valve system is completely unstable and strong noise is produced. In contrast, Figure 14b demonstrates that the servo-valve is stable for the entire sweep frequency band with the high-frequency controller. Moreover, with the high-frequency controller, the second and third harmonics were suppressed, particularly in mid-range frequencies. At very low frequencies, the noise was also reduced.

For those readers familiar with Pelton VibPro™ electronics, it is reasonable to assume that this high-frequency controller will exhibit similar enhancements to the performance of 'stored value' sweeps, as is seen with VibPro internal sweeps. However, a detailed analysis of the new controller's effect on stored value sweeps is outside the scope of this paper, as it entails a much closer look at the intricacies of stored value sweeps.

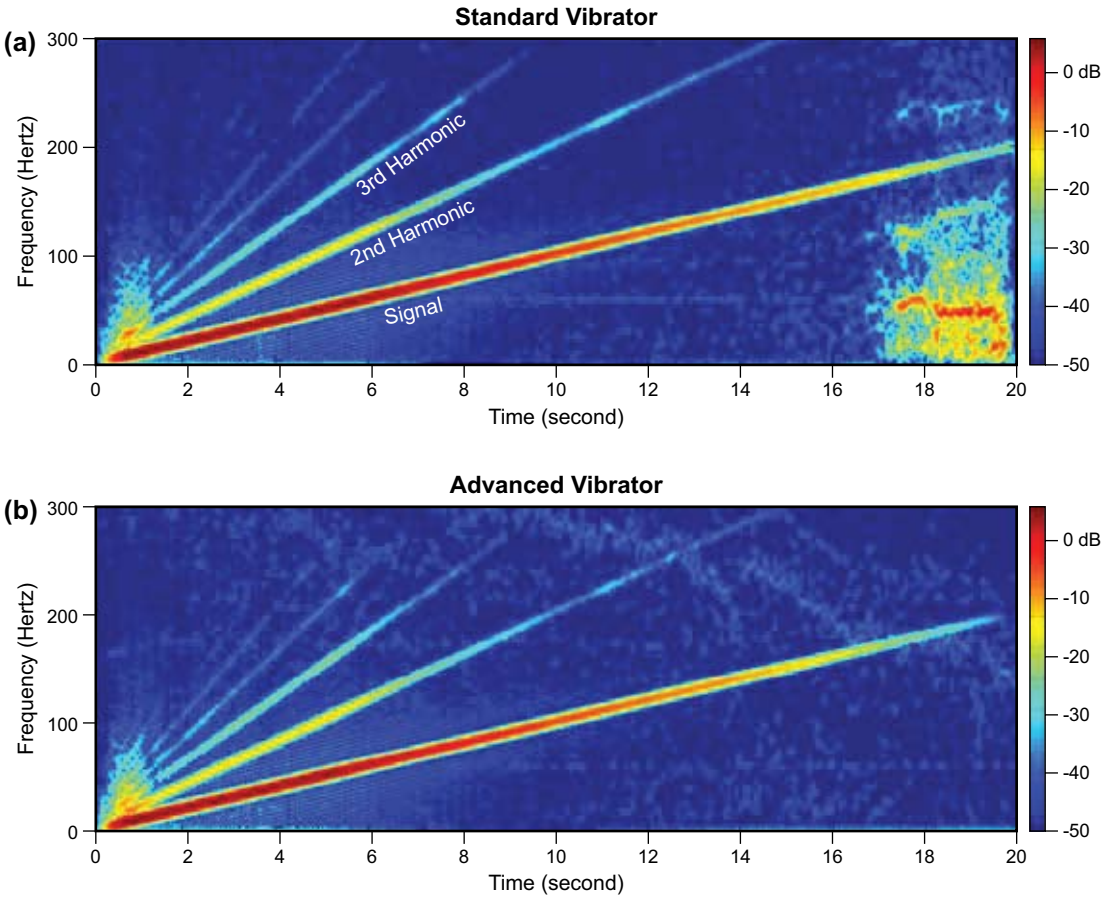

Figure 14: Frequency-time representation of the measured ground force on load cells in Sealy, Texas, USA; (a) Standard AHV-IV vibrator, and (b) AHV-IV vibrator with the new mass and baseplate system. The two vibrators performed a linear sweep from 5 to 200 Hz in 20 seconds at 70% drive force. The fundamental content of the ground forces produced by both vibrators decreases as the sweep frequency increases, implying that the weighted-sum ground force overestimated the actual ground force at high frequencies. It also shows that with the standard controller, at 16 seconds around 160 Hz, the servo-valve system is completely unstable and strong noise is produced. In contrast, the new vibrator with the high-frequency controller for the servo-valve system was stable for the entire swept frequency band. Moreover, the second and third harmonics were suppressed, particularly in mid-range frequencies. At very low frequencies the noise was also reduced.

CONCLUSIONS

Overall, the design implemented in the new mass and new baseplate vibrator produced measurable improvements in the quality of ION's AHV-IV vibrator output signal. These improvements can be achieved in a variety of situations and terrains where difficult loading conditions are common. With the new mass system, ripples and cavitations in the supply pressure, a long-standing problem in vibrator mechanics, were almost completely eliminated. This new baseplate extends the validity of the weighted-sum approximation to a frequency range up to 160 Hz. Moreover, even-order harmonics contained in the ground force were suppressed. These improvements produced a pronounced reduction in the harmonic distortion in the vibrator's signal under various loading conditions. Significant harmonic distortion reduction was achieved when the vibrator was on hard and/or uneven ground, representative of difficult surfaces encountered in desert operations. The high-frequency controller enabled the new mass and baseplate vibrator to achieve a broad frequency bandwidth up to 250 Hz at high-force output.

ACKNOWLEDGEMENTS

I thank ION Geophysical Corporation (previously I/O) for allowing me to publish this work. I am grateful to my colleagues at ION for the testing work. I thank James Hereford for his editing, and I appreciate the valuable comments and suggestions from GeoArabia's reviewers and Editor-in-Chief. The final drafting and design of the paper by GeoArabia Graphic Designer Arnold Egdane is appreciated.

REFERENCES

Al-Ali, M.N. and D.J. Verschuur 2006. An integrated method for resolving the seismic complex near-surface problem. Geophysical Prospecting, v. 54, p. 739-750.

Baetan G. and H. Van Der Heijdan 2008. Improving S/N for high frequencies. The Leading Edge, v. 27, no. 2, p. 144-153.

Bridle, R., N. Barsoukov, M. Al-Homaili, R. Ley and A. Al-Mustafa 2006. Comparing state-of the art near-surface models of a seismic test line from Saudi Arabia. Geophysical Prospecting, v. 54, p. 667-680.

Chapman, W.L., G.L. Brown and D.W. Fair 1981. The Vibroseis system: A high-frequency tool. Geophysics, v. 46, no. 12, p. 1657-1666.

Ley, R., W. Adolfs, R. Bridle, M. Al-Homaili, A. Vesnaver and P. Ras 2006. Ground viscosity and stiffness measurements for near surface seismic velocity. Geophysical Prospecting, v. 54, p. 751-762.

Merritt, H.E. 1967. Hydraulic control systems. John Wiley & Sons, USA, 87 p.

Reust, K.D. 1993. Enhanced Servovalve Technology for Seismic Vibrators. Geophysical Prospecting, v. 41, p. 43-60.

Sallas, J.J. 1984. Seismic vibrator control and the downgoing P-wave. Geophysics, v. 49, no. 6, p. 732-740.

Schinstock, D.E., Z. Wei and T. Yang 2006. Loop shaping design for tracking performance in machine axes. ISA Transactions, v. 45, no. 1, p. 55-66.

Wei, Z. and D.E. Schinstock 2005. Feedforward control strategies for tracking performance in machine axes. Chinese journal of Mechanical Engineering, v. 18, no. 1, p. 5-9.

ABOUT THE AUTHOR

Zhouhong (John) Wei *currently is a Principle Engineer with ION (previously known as I/O) Geophysical Corporation. He received a BSc and a MSc in Mechanical Control Engineering from Gansu University of Technology, Lanzhou, China in 1991 and 1994, respectively. In 2001, John received a PhD in Mechanical Engineering from University of Tulsa, USA. Then, he joined Pelton Company, a subsidiary of ION Geophysical Corporation. His work mainly focuses on seismic vibrator design, control system design for seismic vibrators, servo hydraulic systems and real time DSP embedded systems.*

john.wei@iongeo.com

Manuscript received December 9, 2007

Revised February 2, 2008

Accepted February 12, 2008

Press version proofread by authors March 4, 2008